# Dissipation field asymmetry and intermittency in fully developed turbulence

S. I. Vainshtein
*Department of Astronomy and Astrophysics, University of Chicago, Chicago, Illinois 60637*
(Received 6 December 1999)

Experimental study of high Reynolds number turbulence provides additional evidence that asymmetry of turbulence is related to the intermittency. The refined similarity hypothesis (RSH), on the other hand, connects the intermittency of the longitudinal velocity increments with that of the dissipation field, implying in particular that the dissipation field should be asymmetric as well. The asymmetry of the latter is indeed found in these experiments. In addition, the study of the dissipation field asymmetry provides us with quantitative estimations of the deviations from the RSH.

PACS number(s): 47.27.Ak, 47.27.Jv

## I. INTRODUCTION

Self-similar properties of turbulence, suggested by Kolmogorov (K41) [1], have been intensively studied for a long time. The so-called K41 theory suggests that the probability distribution (PDF) of the longitudinal velocity increments $\Delta_r v$ for different distances $r$ should be self-similar: that is, the conditional probability $p(u|r)$, $u=\Delta_r v/\langle(\Delta_r v)^2\rangle^{1/2}$, is independent of $r$. Basically, this has proved to be the case, although some deviations have been found in high order structure functions (moments of $\Delta_r v$), which are traditionally attributed to the existence of intermittency. A theory incorporating the intermittency, the refined similarity hypothesis (RSH) [2], links the statistics of $\Delta_r v$ with that of the dissipation field $\varepsilon_r$, meaning that now the distribution $p(V|r)$, where $V=\Delta_r v/(r\varepsilon_r)^{1/3}$, is self-similar (independent of $r$) (see also [3]). In spite of quite good experimental validation of RSH [4], [5], there are some deviations from the theory.

One of the issues relevant to these deviations is asymmetric statistics. The asymmetry by itself follows from the Kolmogorov law [6],

$$\langle(\Delta_r v)^3\rangle=-\tfrac{4}{5}\langle\varepsilon\rangle r, \tag{1}$$

which simply manifests an energy transfer to small diffusive scales in fully developed turbulence [7]. It was suggested recently that, in addition, the asymmetry is related to the intermittency [8]. This hypothesis, called the ramp model, has so far been validated experimentally [5,8–11], although there still remain some fundamental questions unanswered, and even not addressed yet. In any case, if confirmed, this hypothesis would provide us with quite a useful tool for studying intermittency. The point here is that traditionally the intermittency has been studied through the high order structure functions: the higher the better. Normally, however, the high order moments are not supported by good statistics. The asymmetry, on the contrary, is manifested already in the low order moments. To begin with, the Kolmogorov law (1) corresponds to the third moment. Experimental studies reveal that the asymmetry is observed in even lower order moments [9].

One may say that the ramp model is consistent with experimental data. Moreover, it has proved to be useful in interpreting a large variety of data, and in studying intermittency, as summarized in [5]. In spite of that, the ramp model still remains only empirical. The main issue is to understand what dynamical processes are behind this connection between the asymmetry and intermittency. Still unable to solve this problem at the present stage (suggesting only some simplified ideas in Sec. VI), we can approach it by addressing the question: How exactly is the asymmetry of turbulence related to the intermittency?

To be more specific, we subdivide this issue into two. First, the Kolmogorov law (1) implies that the velocity increments possess asymmetric statistics, whereas the intermittency is really conspicuous only for the dissipation field. On the other hand, the velocity increments are directly related to the dissipation field via the RSH. Thus, the first goal of this study is to find out if the dissipation field is asymmetric as well.

Second, we might expect that the asymmetry of the PDF of the velocity increments a priori, i.e., following from the Kolmogorov law, should be supported by a vast majority of events, that is, by the PDF core. Moreover, the Kolmogorov law is the only moment of the velocity increments $\Delta_r v$ whose scaling is not subject to the intermittency corrections. Thus, it might seem that the law is unrelated to the intermittency. However, it has long been observed that the $\Delta_r v$ PDF core is not really asymmetric, suggesting that the main asymmetry comes from the tails [12]. Direct comparison of the right and left PDF wings [11] supports this observation. In this paper we study what part of the Kolmogorov law is formed by the core of the PDF, and what part of it is formed by the tails that are responsible for the intermittency of $\Delta_r v$.

We will further refer to a PDF with tails as ''singular.'' This paper is thus devoted to the experimental study of the dissipation field singularities, which are related to the singularities of the $\Delta_r v$ PDF (through the RSH), and manifested in the third moment of $\Delta_r v$ (the Kolmogorov law) through asymmetry.

Section II is introductory as well, giving some basic information about asymmetry aspects of turbulence, and, in particular, about the ramp model. It is shown in Sec. III that the intermittency of the dissipation field is asymmetric. The direct connection between asymmetry, dictated by the Kolmogorov law, and the tail parts of the velocity increment PDF is studied in Sec. IV. Section V is devoted to studying the connection between these two fields—the dissipation

 

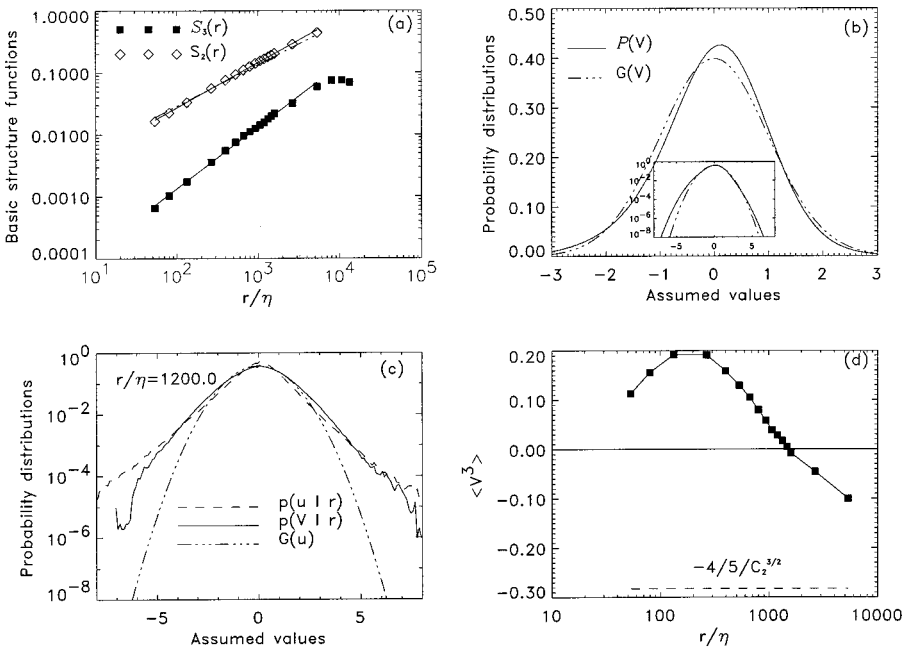


FIG. 1. (a) The Kolmogorov law $\mathcal{S}_3(r)$ and second order structure function $S_2(r)$. The straight solid lines correspond to linear fitting, and dot-dashed lines to $S_2(r)=C_2(\langle\varepsilon\rangle r)^{2/3}$. (b) ''Ideal'' PDF for $V$ compared with Gaussian $G(V)$. The inset shows these two distributions for larger values. (c) Several typical PDF's, compared with Gaussian $G(u)$ with the same standard deviation as $p(u|r)$. (d) The third moment of $V$, which is compared with the theoretical value $-(4/5)/C_2^{3/2}$.

field and the velocity increments—with emphasis on the asymmetry of statistics. The main conclusions are given in Sec. VI.

## II. DESCRIPTION OF THE METHOD AND NOTATIONS

We used $10\times10^6$ points of atmospheric data from Yale University, with an estimated Taylor microscale Reynolds number of 9540. The data are treated in the spirit of the Taylor hypothesis, that is, the time series is treated as a one-dimensional cut of the process (for more detail, see [10,5]).

We study the statistics of the velocity increments $\Delta_r v$ and of the dissipation field $\varepsilon_r$ for different distances, from $r/\eta=53.33$ to $r/\eta=13\,333.3$ (in terms of the Kolmogorov scale $\eta$). We denote structure functions

$$\mathcal{S}_n=\langle(\Delta_r v)^n\rangle,$$

and generalized structure functions

$$S_q(r)=\langle|\Delta_r v|^q\rangle.$$

It can be seen from Fig. 1(a) that $\mathcal{S}_3(r)$, i.e., the Kolmogorov law (1), can been fitted for a somewhat shorter scale range, from $r/\eta=53.33$ to $r/\eta=5333.33$, that is, for two decades. The exponent is $0.992\pm0.018$, quite close to the unity required for the Kolmogorov law (if we remove the right end point taken for the fitting, then the exponent deviates slightly more from unity). This range of distances, where the Kolmogorov law fits satisfactorily, we will consider as ''standard,'' and all other measurements were provided in this range. In particular, we calculated $\langle\varepsilon\rangle$ from this experimental plot, as follows from Eq. (1). This value of $\langle\varepsilon\rangle$ can be substituted into the second moment,

$$S_2(r)=C_2(\langle\varepsilon\rangle r)^{2/3}, \tag{2}$$

with Kolmogorov constant $C_2=2\pm0.4$; see, e.g., [3]. It can be seen from Fig. 1(a) that the experimental $S_2(r)$ in our range of distances is quite close to Eq. (2), illustrating self-consistency of the measurements. The real slope of $S_2(r)$, obtained by fitting, is slightly steeper, consistent with the well known observation that the exponent is somewhat bigger than 2/3: namely, the exponent $\zeta_2=0.72\pm0.01$, quite close to $\zeta_2=0.71$ obtained in [13].

The local rate of dissipation $\varepsilon$, and correspondingly the dissipation field $\varepsilon_r$, are also understood as one dimensional,

$$\varepsilon=15\nu(\partial_x v_x)^2, \quad \varepsilon_r=\frac{1}{r}\int_{x-r/2}^{x+r/2}\varepsilon(x)dx, \tag{3}$$

which is sometimes called pseudodissipation. It was reiterated recently that pseudodissipation provides useful information, especially because it is measured for very high Reynolds numbers [14].

According to the refined similarity hypothesis [2],

$$\Delta_r v=\sqrt{C_2}V(\varepsilon_r r)^{1/3}, \tag{4}$$

where $V$ is a random function statistically independent of $\varepsilon$. The prefactor in Eq. (4) ensures that the second moment corresponds to the experimental value (2), provided $\langle V^2\rangle\approx1$. We will use Eq. (4) in the dimensionless form,

$$u=Vy, \tag{5}$$

where

$$u=\frac{\Delta_r v}{\sqrt{C_2}(\langle\varepsilon\rangle r)^{1/3}}, \quad y=\left(\frac{\varepsilon_r}{\langle\varepsilon\rangle}\right)^{1/3}.$$

Thus, $u$ is defined in such a way that $\langle u^2\rangle$ should be close to unity. This is indeed the case, as follows from Fig. 1(a), or when recovering the second moments from experimental PDF's, i.e., calculating $\int u^2 p(u|r)du$ from experimental $p(u|r)$.

Thus, according to the RSH, $V$ is a nonsingular universal function, with standard deviation close to unity. As $V$ and $y$ are statistically independent, and $y$ is non-negative, it follows that $\langle V\rangle=0$. On the other hand, the third moment of $V$ is defined by the Kolmogorov law (1), and by definition (4), $\langle V^3\rangle=-(4/5)/C_2^{3/2}$. These two requirements, $\langle V\rangle=0$ and $\langle V^3\rangle<0$, suggest that $p(-V)>p(V)$ for large $|V|$, and, in order to balance this to make the first moment vanish, $p(-V)<p(V)$ for small $|V|$. However, as the corresponding PDF is nonsingular, the ''large'' values of $|V|$ are in fact moderate, say, $1<|V|<3$. In other words, both asymmetries mentioned above should be inside the PDF core. Figure 1(b) depicts this ''ideal'' PDF for $V$, denoted by $\mathcal{P}(V)$. It is constructed as a sum of two Gaussian distributions with standard deviations close to unity (to avoid any tails, because the function should be nonsingular). This function thus satisfies

$$\int \mathcal{P}(V)dV=1, \quad \int \mathcal{P}(V)VdV=0,$$

$$\int \mathcal{P}(V)V^2dV=1, \quad \int \mathcal{P}(V)V^3dV=-\frac{4}{5}\frac{1}{C_2^{3/2}}.$$

The function does not contain tails: its deviation from Gaussian form at large values is insignificant. However, at the core, it has the needed asymmetry: $\mathcal{P}(-V)>\mathcal{P}(V)$ for $1<|V|<2$, say, and $\mathcal{P}(-V)<\mathcal{P}(V)$, for $|V|<1$. This function will be used to compare with experimental PDF's.

As to the PDF for $u$, it is expected both from K41 and the RSH that the asymmetry will be qualitatively the same as for $\mathcal{P}(V)$. The only difference is that, because of the presence of a singular process $y$ in Eq. (5), the velocity increments $u$ are singular as well, i.e., there are tails in $p(u|r)$. However, as $y$ ''does not know'' about the sign of $u$, being always non-negative, this asymmetry should not be noticeable in the tails. In other words, the asymmetry should be manifested mainly in the cores of the PDF, rather than in the tails. This difference (i.e., that the process $V$ is nonsingular, while $u$ is singular) is expected to completely disappear for the third moment $\mathcal{S}_3(r)$. Indeed, according to Eq. (4), the intermittency is irrelevant for this moment, corresponding to the Kolmogorov law. In other words, this moment does not vanish only due to asymmetry. Thus, an important test for the RSH is to check if this is indeed the case. In order to do this, we will consider cumulative moments,

$$\langle u^3\rangle_c=\int_{-c}^{c}u^3p(u|r)du, \quad \langle V^3\rangle_c=\int_{-c}^{c}V^3\mathcal{P}(V)dV, \quad (6)$$

and what we may call tail moments,

$$\langle u^3\rangle_t=\int_{-\infty}^{-t}u^3p(u|r)du+\int_{t}^{\infty}u^3p(u|r)du,$$

$$\langle V^3\rangle_t=\int_{-\infty}^{-t}V^3\mathcal{P}(V)dV+\int_{t}^{\infty}V^3\mathcal{P}(V)dV. \quad (7)$$

We denote

$$\mathcal{S}_3^{(c)}(r)=C_2^{3/2}\langle\varepsilon\rangle r\langle u^3\rangle_c, \quad \mathcal{P}^{(c)}(r)=C_2^{3/2}\langle\varepsilon\rangle r\langle V^3\rangle_c, \quad (8)$$

so that, by definition (4), $\mathcal{S}_3^{(c\to\infty)}(r)=\mathcal{S}_3(r)$, and, according to the RSH, $\mathcal{P}^{(c\to\infty)}(r)=\mathcal{S}_3(r)$. Analogously,

$$\mathcal{S}_3^{(t)}(r)=C_2^{3/2}\langle\varepsilon\rangle r\langle u^3\rangle_t, \quad \mathcal{P}^{(t)}(r)=C_2^{3/2}\langle\varepsilon\rangle r\langle V^3\rangle_t, \quad (9)$$

so that $\mathcal{S}_3^{(t=0)}(r)=\mathcal{P}^{(t=0)}(r)=\mathcal{S}_3(r)$. As mentioned above, the intermittency is irrelevant for this moment, and therefore one would expect that the main contribution to the moment would be given by the majority of events, that is, by the PDF core. In other words, qualitatively, both $\mathcal{S}_3^{(c)}(r)$ and $\mathcal{S}_3^{(t)}(r)$ are expected to behave like $\mathcal{P}^{(c)}(r)$ and $\mathcal{P}^{(t)}(r)$. So one of the tests of the RSH would be to compare the experimental $\mathcal{S}_3^{(c)}(r)$ and the $\mathcal{S}_3^{(t)}(r)$ with ''ideal'' behavior given by $\mathcal{P}^{(c)}(r)$ and $\mathcal{P}^{(t)}(r)$.

According to the RSH, $y$ and $V$ are statistically independent; in particular, $y$ should not ''know'' about the sign of $V$ (and, therefore, it should be uncorrelated with the sign of $u$). We denote by $y^{\pm}$ the dissipation field corresponding to $u^{\pm}$. We will deal with conditional probabilities, $p(y^{\pm},\pm1|r)=p(y,u/|u|\,|r)$, so that only $p(y^+,1|r)\equiv p(y^+|r)$ and $p(y^-,-1|r)\equiv p(y^-|r)$ do not vanish, while $p(y^+,-1|r)=p(y^-,1|r)=0$. These PDF's are thus normalized to satisfy

$$\int_0^\infty p(y^+|r)dy^+ + \int_0^\infty p(y^-|r)dy^-=1.$$

Statistical independence between $y$ and $V$ means that the PDF's are symmetric, $p(y^+|r)=p(y^-|r)$, and therefore

$$\int_0^\infty p(y^+|r)dy^+=\int_0^\infty p(y^-|r)dy^-=\tfrac{1}{2}.$$

In particular, if $\omega=\partial_x v(x)$ is Gaussian, then the distribution for $y=\varepsilon^{1/3}/\langle\varepsilon^{1/3}\rangle^{1/2}$ has the form

$$G_\omega(y|r)=\frac{3y^{1/2}}{2\sqrt{2\pi}}e^{-y^3/2}, \quad (10)$$

which differs from Eq. (23) of [5] by a factor 1/2, because the normalization is now different.

Another way to study the dissipation asymmetry is to consider two sets,

$$\varepsilon^{\pm}(x)=\frac{1}{2}\left(\varepsilon(x)\pm\varepsilon(x)\frac{\partial_x v_x}{|\partial_x v_x|}\right). \quad (11)$$

It is clear that these two sets do not intersect with each other, and therefore it is possible to introduce separate measures,

$$\mu_r^{\pm}=\int_{x-r/2}^{x+r/2}\varepsilon^{\pm}(x)dx, \quad (12)$$

cf. Eq. (3). In particular, we will study moments of these measures, defining the generalized dimensions as follows:

$$\langle(\overline{\mu_r^{\pm}})^q\rangle \sim r^{\xi_q^{\pm}} = r^{-(1-D_q^{\pm})(q-1)}, \tag{13}$$

where

$$\overline{\mu_r^{\pm}} = \frac{\mu_r^{\pm}}{r}.$$

The experimental studies of the PDF's show some deviations from the ''ideal'' behavior described above. Figure 1(c) depicts typical experimental PDF's. These deviations can be summarized as follows: (1) There is asymmetry of the $p(u|r)$, noticeable in the tails; namely, the left wing is definitely higher than the right [11]. (2) The PDF for $V$ has tails as well, the right-hand wing reaching values of $p(u|r)$, and the left-hand wing is still above a Gaussian distribution, and typically above $\mathcal{P}(V)$, although not much [5]. (3) The right-hand wings of $p(V|r)$ are higher than the left-hand wings, i.e., the asymmetry of $p(V|r)$ is opposite to that of the ''ideal'' PDF for $V$, and opposite to the asymmetry of $p(u|r)$. This observation is supported by direct measurement of odd moments. Thus, as was shown in [5], $\langle V^3\rangle$ is often positive. Figure 1(d) illustrates this result once again. The difference between this plot and corresponding plots in [5] is that the plots in [5] depict different data samples, normalized separately, so they can be considered as separate experiments, whereas all present measurements correspond to the processing of all available data.

Finally, we summarize what the ramp model predicts. In essence, the ramp model suggests that the asymmetry is manifested not so much at the cores of the PDF's but rather at the tails, i.e., the asymmetry is by itself singular, and thus it is directly related to the intermittency. More specifically, in terms of central moments, the above means the following. Let $a^{\pm}=(|a|\pm a)/2$, where $a$ is some random process. If applicable for this process, the ramp model suggests that

$$\begin{aligned} &\langle(a^-)^q\rangle > \langle(a^+)^q\rangle \quad \text{for} \quad q>1, \\ &\langle(a^-)^q\rangle < \langle(a^+)^q\rangle \quad \text{for} \quad q<1. \end{aligned} \tag{14}$$

In addition, if the moments of $a^{\pm}$ possess any scaling, $\langle a^{\pm}\rangle^q \sim r^{\xi_q^{\pm}}$, as in Eq. (13), then

$$\begin{aligned} &\xi_q^+ > \xi_q^- \quad \text{for} \quad q>1, \\ &\xi_q^+ < \xi_q^- \quad \text{for} \quad q<1, \end{aligned} \tag{15}$$

which, according to Eq. (13), corresponds to

$$D_q^- < D_q^+ . \tag{16}$$

In particular, for the velocity increments, the (negative) skewness is defined mostly by the tails of the velocity increment PDF, and the core possesses opposite symmetry, i.e.,

$$\begin{aligned} &p(u^+|r) < p(u^-|r) \quad \text{for large} \quad u^{\pm}, \\ &p(u^+|r) > p(u^-|r) \quad \text{for the core.} \end{aligned} \tag{17}$$

## III. ASYMMETRY OF THE DISSIPATION FIELD

### A. Asymmetry of $p(y^{\pm}|r)$

The results of the measurements can be summarized as follows. First, all the measured $y^{\pm}$ distributions are singular, being well above $G_{\omega}$ [Eq. (10)]. Second, the strength of the singularity of both $\pm$ dissipation fields is less than that of $\Delta_r v$: the PDF's for $y^{\pm}$ are noticeable below those for $u^{\pm}=(|u|\pm u)/2$, for values, say, greater than 2. In addition, for large distances, there is always a cutoff value for the $y^{\pm}$ distributions, e.g., there are no events with $y^{\pm}>6$, say, while there are larger values of $u^{\pm}$, up to the measured limit of 8 (cf. [5]). These trends can also be seen from Fig. 2, illustrating these distributions for four distances. Third, for values, say, greater than 2, the PDF's for $y^-$ are typically higher than those for $y^+$ (some examples are given in Fig. 2), in accordance with the ramp model (see the end of Sec. II).

Note, however, that this excess is manifested only as a trend: in contrast to the $u^{\pm}$ asymmetry, the latter being really systematic, like a law. Indeed, $p(u^-,|r)>p(u^+,|r)$ for $u>2$, and for all distances [10]. Nevertheless, this trend is also obvious, and that can be seen from the behavior of the fourth moment $\langle(y^{\pm})^4\rangle$ depicted in Fig. 3(a). It definitely shows that $\langle(y^-)^4\rangle>\langle(y^+)^4\rangle$, for all distances. Returning to the PDF in Fig. 2: an occasional prevalence of $p(y^+|r)$ over $p(y^-|r)$ for large $y^{\pm}$ can be attributed to the fact that we are dealing with the very end of the distribution function, that is, with very rare events, subject to strong fluctuations (not so with the $u^{\pm}$ distributions; as seen from Fig. 2, the studied values are far from the end of the distributions). Therefore, it makes sense to study the cores of these distributions, where statistics are good. According to the ramp model, the asymmetry at small values is opposite to that at large ones, that is, for these values, $p(y^+|r)>p(y^-|r)$ [cf. Eq. (17)]. The experimental PDF is indeed in agreement with this expectation, as seen from the insets to Fig. 2. The insets depict some selected distances; it is noteworthy, however, that all the PDF's from the data we analyzed look this way: $p(y^+|r)>p(y^-|r)$ for $y^{\pm}\leqslant 1$.

In order to show it quantitatively, we measured the relative number of events with $y\leqslant 1$ (a sort of box counting), namely, $N^{\pm}=\int_0^1 p(y^{\pm}|r)dy^{\pm}$. Figure 3(b) shows that indeed $N^+>N^-$, for all the studied data.

Another presentation of this asymmetry is provided by the zeroth moment. According to the definition given in Sec. II, the zeroth moment simply corresponds to the box counting for the distributions $y^{\pm}$, or, equivalently, for $u^{\pm}$ distributions. If the process were symmetric, then

$$p(y^+>0|r)=p(y^->0|r)=\tfrac{1}{2},$$

that is, the probability of $u$ being positive is the same as the probability of $u$ being negative, and equal to 1/2 (we excluded values $u=0$ from the data, considering them spurious; see Sec. IV A below). According to the ramp model, we expect that the negative parts of the $u$ distribution will occupy less space than the positive parts [see Eq. (14) for $q=0$]. Figure 3(c) shows that this is indeed the case. By definition, $p(y^+>0|r)+p(y^->0|r)=1$, that is, if the negative distribution occupies $f$'s fraction of the experimental interval ($f<1/2$), then the positive part occupies the rest, i.e., (1

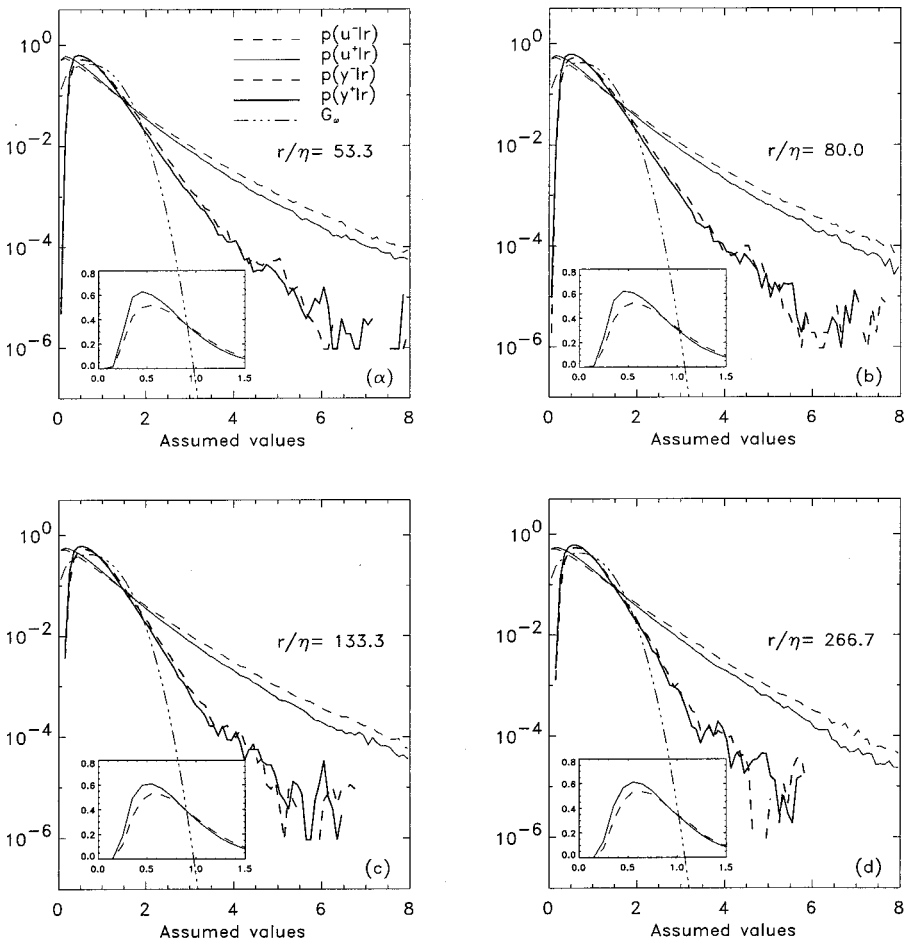


FIG. 2. Comparison of the PDF's for the velocity increments $\Delta_r v$ with those for the dissipation field, separately for $\pm$ distributions, for four distances. The $y^-$ distribution is typically above the $y^+$ distribution for large values. Both these distributions are well above $G_\omega$—a distribution for $\varepsilon$ if $\partial_x v(x)$ is Gaussian. The insets give the same PDF's, but for smaller values. $p(y^+|r)$ is depicted by the solid line and $p(y^-|r)$ by the dashed line. It can be seen that $p(y^+|r) > p(y^-|r)$ for $y \leqslant 1$, and that feature appears in all the data we studied. All the distances are given in terms of the Kolmogorov microscale $\eta$.

$-f$)'s fraction. Therefore, if there is some scaling for $f, f(r) = a_0 r^{\xi 0}$, then the negative part may be considered as singular, and the corresponding Kolmogorov capacity can be estimated. In that case, the positive part is trivially related to the negative part, namely, it is $= 1 - a_0 r^{\xi 0}$, which is not a power law, and therefore not interesting. The Kolmogorov capacity $D_0$ is defined through the formula

$$f(r) = a_0 r^{1 - D_0}, \tag{18}$$

which is a particular case of Eq. (13).

It is apparent from Fig. 3(c) that the fraction $f(r)$ is indeed systematically increasing with growing $r$, as suggested by expression (18), provided $D_0 < 1$. The fitting of the box counting of this distribution to a straight line results in $D_0$

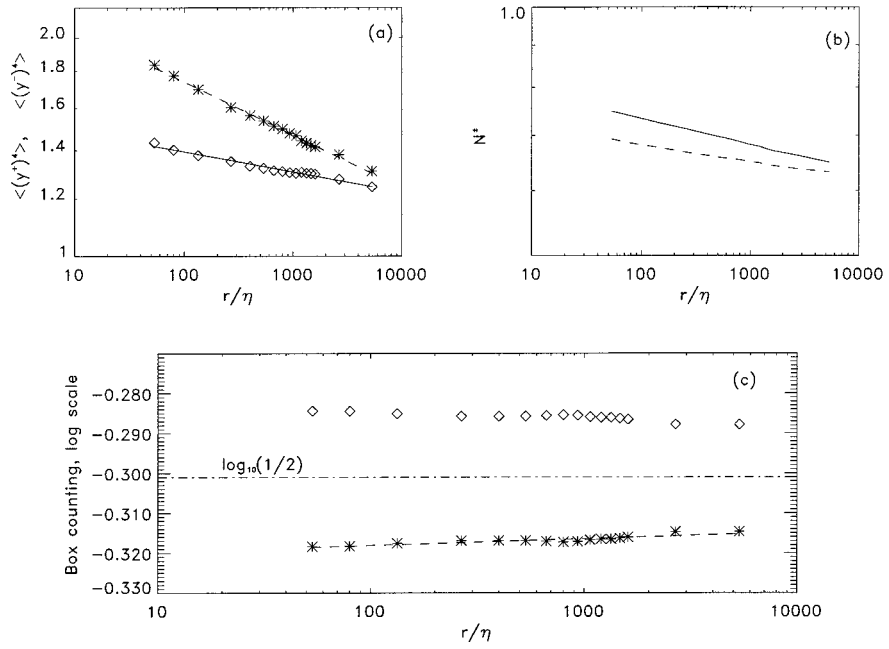


FIG. 3. Different moments of the $y^\pm$ distribution. Both axes in all panels are in logarithmic scale. (a) presents $\langle (y^+)^4 \rangle$, asterisks, and $\langle (y^-)^4 \rangle$, diamonds. The points are fitted with straight lines. The inequality $\langle (y^-)^4 \rangle > \langle (y^+)^4 \rangle$ is always satisfied. In addition, these lines have different slopes, corresponding to $D_4^- < D_4^+$. (b) The number of events $N^\pm$ with $0 \leqslant y^\pm \leqslant 1$; $N^+$, solid line, $N^-$ dashed line. It can be seen that the inequality $N^+ > N^-$ is always satisfied. (c) Box counting (asterisks for the negative and diamonds for the positive distributions) and fitting for the negative distribution.

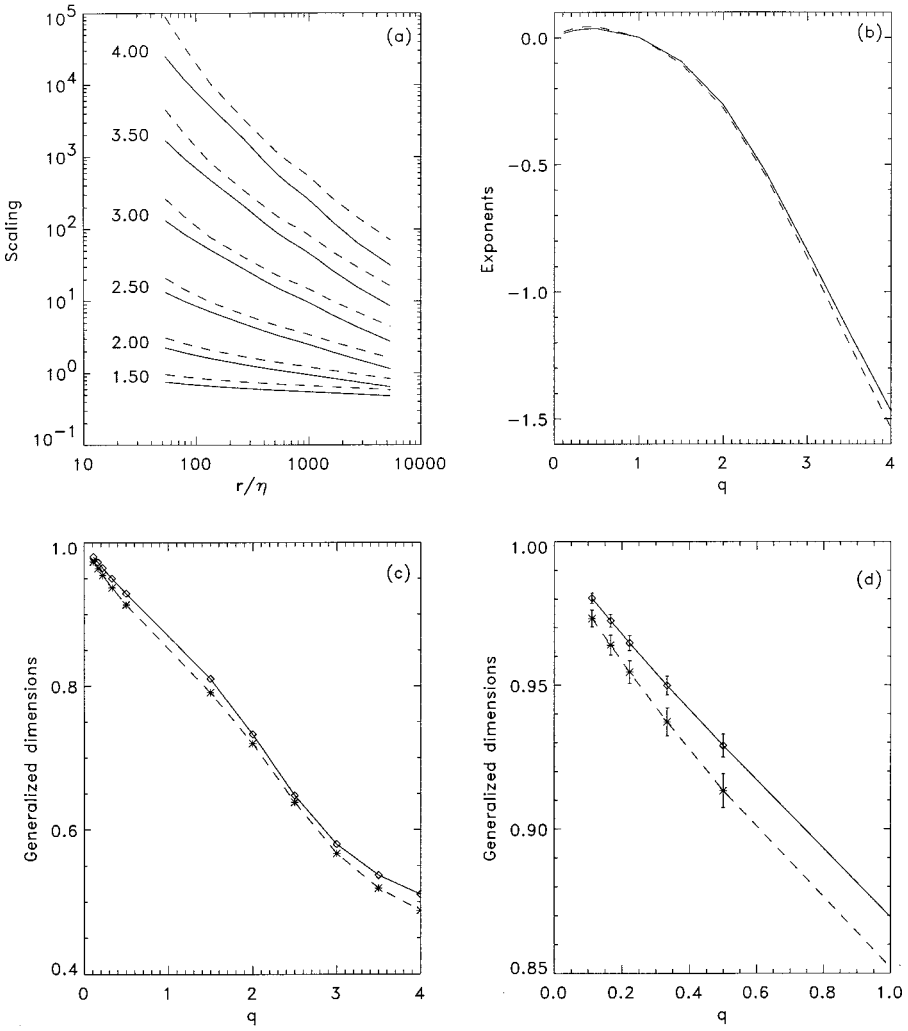


FIG. 4. (a) Different moments of the two sets Eq. (11); the numbers on the left give the values of $q$. (b) Exponents $\xi_q$. (c) The dimensions calculated according to Eq. (13). (d) Same for smaller $q$. In all panels, solid lines correspond to the + distribution and dashed lines to the − distributions.

$=0.9983\pm0.0002$. As the generalized dimensions are decreasing monotonically with growing $q$ [15], a nontrivial Kolmogorov capacity $D_0^- < 1$ means that all the dimensions are nontrivial, $D_q^- < 1$. Recall that the statistics for the zeroth moment are as good as possible. In spite of the fact that the deviation from unity is tiny, $1 - D_0 = 0.0017$, it is still considerably larger than the error, 0.0002. In addition, the nontrivial Kolmogorov capacity has already been observed [10], although for substantially smaller distances, for which the slope is steeper and therefore the Kolmogorov capacity deviates more strongly from unity. It is hard to compare these two measurements, though. They correspond to two different processes (pipe turbulence in [10] and atmospheric turbulence in the present study), and because the measurements in [10] correspond to a range between the dissipation and inertial ranges, whereas all the distances here are well inside the inertial range. Nevertheless, in view of the small deviation of the Kolmogorov capacity from unity in our ''standard'' range of distances, there is no guarantee that some systematic errors are not involved, making it nontrivial. At the same time, the asymmetry itself, i.e., that $f(r) < 1/2$, consistent with Eq. (14), is clearly seen from Fig. 3(c).

### B. Asymmetry of the $\mu_r^{\pm}$ measures

The most straightforward approach to studying the asymmetry and related intermittency is to analyze the two sets $\varepsilon^{\pm}$ defined in Eq. (11). Figure 4(a) illustrates some of the studied moments $\langle(\overline{\mu_r^{\pm}})^q\rangle$. It is clear that $\langle(\overline{\mu_r^-})^q\rangle > \langle(\overline{\mu_r^+})^q\rangle$, in accordance with the ramp model [see Eq. (14)].

Panel (b) of Fig. 4 confirms Eq. (15), although the two curves are quite close to each other. Direct calculation of the generalized dimensions, defined in Eq. (13) [panels (c) and (d)] shows that Eq. (16) is satisfied as well. As seen from panel (d), the error bars do not overlap for small $q$, in spite of the fact that the difference between + and − dimensions is small. The statistic here is reliable, because the moments are of low order. For $q \geqslant 2.5$ the error bars do overlap, so that one can claim that inequality (16) is satisfied at these $q$'s only as a trend. We should keep in mind, however, that these moments are in effect of relatively high orders, corresponding via the RSH to velocity increments of order $q = 7.5$ or higher.

## IV. ASYMMETRY OF THE PDF CORE

### A. The PDF for $u$: problem of zero values

According to Eq. (17), the PDF core for $u$ is expected to possess an asymmetry opposite to that at the tails. In spite of good statistics at the core this asymmetry was not really observed. Usually, the PDF has a distinctive peak at zero, which might obscure the asymmetry.

The question of the behavior of the PDF at $u = 0$ is important by itself. Indeed, the PDF may have a $\delta$ function at

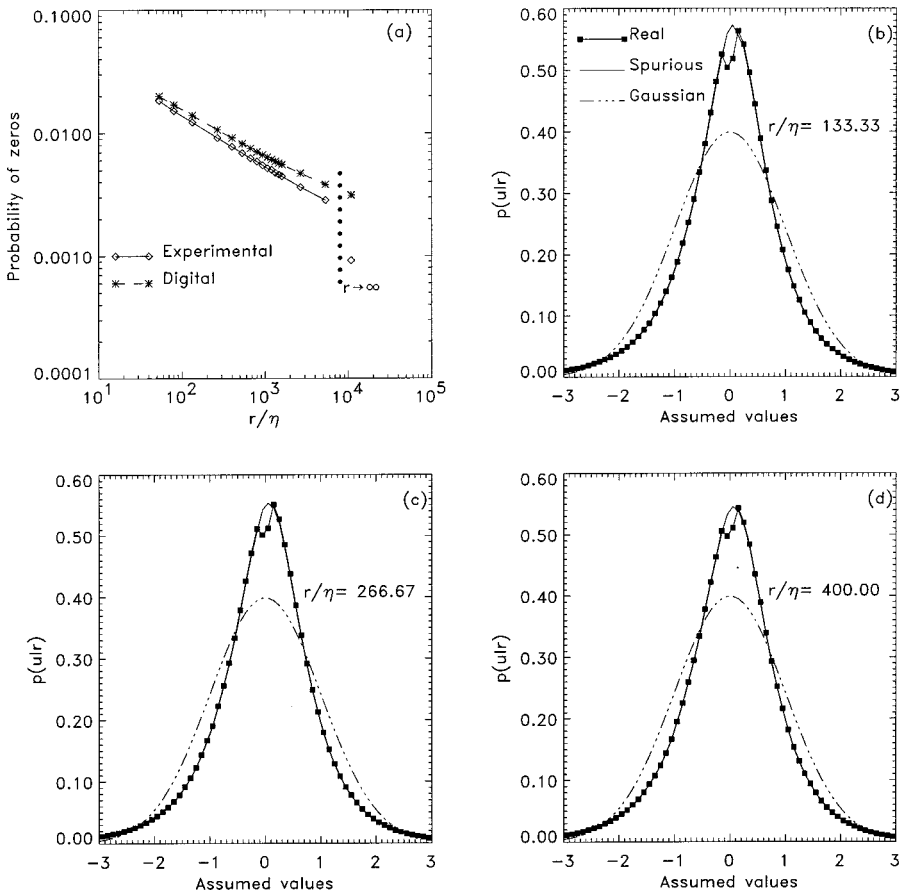


FIG. 5. (a) The probability of zeros: experimental and digital, according to Eq. (19). (b)–(d) illustrate the PDF cores for different distances, with and without additional zeros at $u=0$. The measured PDF's do contain zeros, but we consider them spurious.

the origin, i.e., $p(u|r)\sim\delta(u)$, which would mean a nontrivial Kolmogorov capacity (see, e.g., [16]). The experimental PDF's seem to suggest that this is indeed the case. The histograms $H(u|r)$ are constructed for the interval $-8\leqslant u\leqslant 8$, with bin size $\Delta=0.1$. For all bins, we have $H(m\Delta<u<(m+1)\Delta|r)>0$, where $m=0,\pm1,\pm2,\ldots$, whereas $H(m\Delta|r)=0$, as it should for any continuous distribution. The only exception is $H(0,|r)$, which always contains a considerable amount of elements (i.e., $H(0,|r)\gg 1$). These zeros could be simply spurious, though. Indeed, the raw data are given in (four digit) integers, so that the differences between two data points (calculated in constructing the structure functions) have a finite probability of being zero. Denoting by $p(n_i)$ the probability that the data assume the value $n_i$, then the probability of zero will read

$$p(0|r)=\frac{H(u=0|r)}{N}=\sum_i p(n_i)p(n_i|n_i,r), \qquad (19)$$

where $N$ is the number of events, and $p(n_i|n_j,r)$ is the conditional probability that the second data point separated by distance $r$ assumes the value $n_j$ provided that the first data point assumes the value $n_i$. For $r\to\infty$ the two events are statistically independent, meaning that $p(n_i|n_j,r\to\infty)=p(n_i)$. If, e.g., the distribution is homogeneous, $p(n_i)=1/n$, $n$ being the number of available numbers, then $p(0|r\to\infty)=1/n$ as well. In practice, this probability is not that small; and for finite distances, where the two data points are correlated, the probability is even higher. The probability $p(0|r)$ according to Eq. (19) was estimated using experimental probabilities on the right-hand side of Eq. (19). The resulting probability is called ''digital'' and depicted in Fig. 5(a). The figure also compares this probability with direct measurements of the number of zeros. The real probability $p(0|r)$ is always below the digital, and therefore the measured numbers $H(0,|r)$ are unreliable.

These numbers, however, give a considerable contribution to the histogram at $-0.1<u<0.1$. If we remove this contribution, thus considering it spurious, the histograms change. Figures 5(c)–(d) show the new PDF's and compare them with the old. One can clearly see the ''needed'' asymmetry of the cores, and that the spurious (including the zeroth) PDF confuses the asymmetry, looking much more symmetric than it should. Thus, we consider the zeros appearing at the origin of the PDF for $u$ as spurious. Another independent confirmation of such an approach is that the Kolmogorov capacity of the $u$ process is always observed as trivial (see, e.g., [17]), unlike the $u^-$ processes, which, as argued in Sec. III A, might possess a nontrivial Kolmogorov capacity.

### B. The third order moment

It can be expected that this moment is of low order, concerning essentially the core of the PDF, while the tails are not supposed to give a substantial contribution. This is definitely true for the generalized structure function $S_3(r)$. However, the structure function $\mathcal{S}_3(r)$ might behave differently, because it does not vanish only due to asymmetry, and the latter is manifested at the tails [10]. In order to verify this, we study the third cumulative moment, depicted in Fig. 6. As the upper limit $c$ grows, the cumulative moment should approach

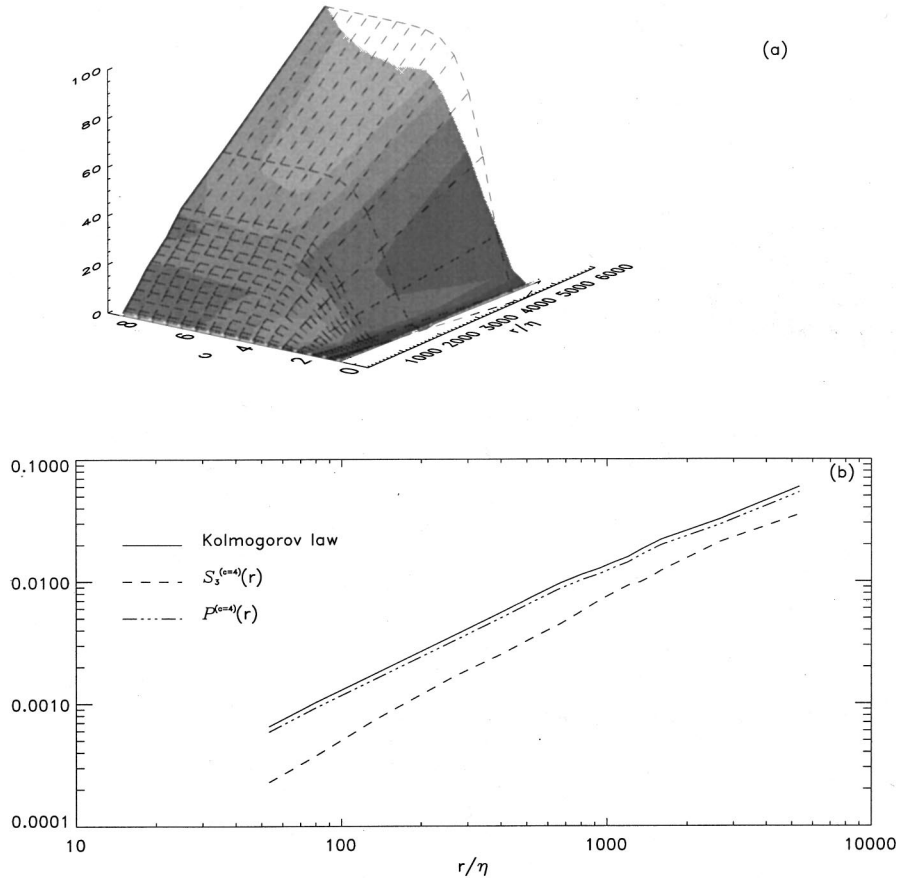


FIG. 6. (a) Comparison of $\mathcal{S}_3^{(c)}(r)$ (shaded surface) with $\mathcal{P}^{(c)}(r)$ (dashed surface) as functions of $r/\eta$ and $c$. Both functions approach the Kolmogorov law at large $c$ (bold line). (b) Same comparison for $c=4$.

the Kolmogorov law [see the definition Eq. (6)]. It can be seen from Fig. 6 that the ''ideal'' cumulative moment $\mathcal{P}^{(c)}(r)$ approaches the Kolmogorov law substantially faster than the measured structure function. In particular, $c=4$ corresponds to 99.9968% of events for a Gaussian distribution, and between 99.459% and 99.796% for experimental events. As seen from panel (b), even for this overwhelming majority of events, the cumulative moment of the experimental PDF is still far from the Kolmogorov law, while $\mathcal{P}^{(c=4)}(r)$ almost coincides with the law. It is also evident that $\mathcal{S}_3^{(c=4)}(r)$ is closer to the law for large distances, where the intermittency is lower. The same trends are apparent from Fig. 7, where cumulative moments as functions of $c$ for different distances are depicted. The moment $\mathcal{P}^{(c)}(r)$ is almost saturated at $c=4$, reaching the Kolmogorov law, whereas $\mathcal{S}_3^{(c)}(r)$ saturates substantially more slowly. Due to inverse asymmetry at small values, the cumulative functions are positive for small $c$, this positive maximum being more pronounced for $\mathcal{P}^{(c)}(r)$. It can be noticed also that, as the distance increases, the difference between these two distributions becomes less pronounced.

The situation with the tail moments (7) is opposite. It is clear from Fig. 8(a) that at $t>2$, where the contribution of the tails becomes more important and the core is essentially cut off, the experimental $\mathcal{S}_3^{(t)}(r)$ is many orders of magnitude higher than $\mathcal{P}^{(t)}(r)$. The Kolmogorov law is achieved at the smallest $t$, where the whole PDF contributes. As seen from Fig. 8(b), even for $t=4$, corresponding to $\approx 0.3\%$ of events, the tail moment is reasonably close to the law, while $\mathcal{P}^{(t=4)}(r)$ is substantially further away from it. Note that this time $\mathcal{S}_3^{(t=4)}(r)$ is even closer to the Kolmogorov law for small $r$, as opposed to $\mathcal{S}_3^{(c=4)}(r)$, which is closer to the law for large $r$. The reason is the same: the intermittency is more pronounced at small $r$, and so is the asymmetry. Figure 9 compares $\mathcal{S}_3^{(t)}(r)/|\mathcal{S}_3^{(t=0)}(r)|$ with $\mathcal{P}^{(t)}(r)/|\mathcal{P}^{(t=0)}(r)|$ as functions of $t$ for different distances. At $t=0$ the tail moments coincide with the Kolmogorov law, and therefore the curves approach $-1$, reflecting the fact that the skewness is negative. At $t\geqslant 4$, that is, for quite rare events, the ''ideal'' moment is almost zero, as it should be, whereas the observed tail moments present a considerable fraction of the Kolmogorov law. As in Fig. 7, the difference between ''ideal'' behavior and observed tail moments is decreasing with growing distances, which we attribute to the decreasing role of intermittency for large $r$. Finally, due to the inverse asymmetry at small values, there is a deep minimum in the curves for ''ideal'' moments (corresponding to the positive parts in the cumulative moments in Fig. 7, mentioned above), and a less pronounced minimum in the experimental curves. Indeed, for $t=2$, say, the positive values that prevail at these values are subtracted, resulting in an increase of the absolute values of negative skewness. The difference between the ''ideal'' behavior and experimental curves at the cores (more pronounced maximums for cumulative moments and minimums for the tail moments) is directly related to the fact that the inverse asymmetry of $\mathcal{P}$ is quite noticeable at the core in Fig. 1(b), while it is not that conspicuous for the experimental PDF's depicted in Figs. 5(b)–5(d), even after removing the zeros at the origin, as explained in Sec. IV A. This happens because both typical and inverse asymmetry are mani-

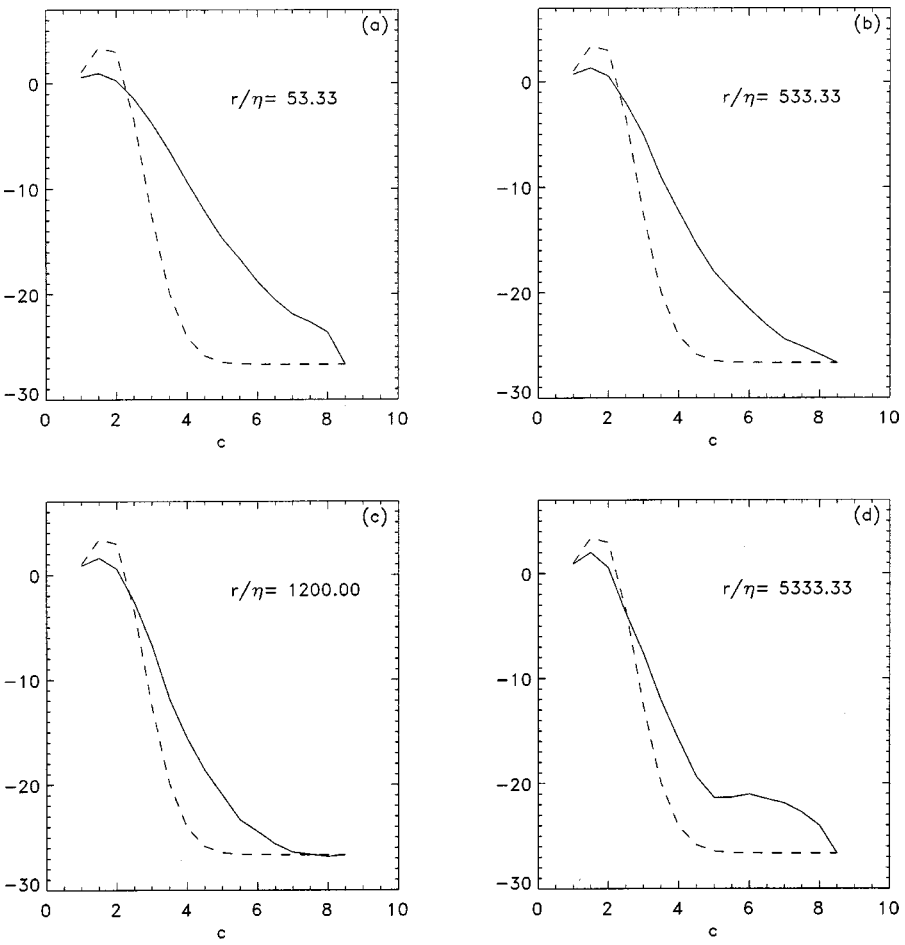


FIG. 7. Same as in Fig. 6, but for fixed distances, while the cumulative moments are depicted as functions of $c$. Solid line corresponds to the experimental PDF and dashed to the ''ideal'' PDF. For illustrative purposes all the curves are normalized to their initial values (at $c=0$).

fested in the core of $\mathcal{P}$ [and indeed they both can be seen in Fig. 1(b)], whereas the experimental PDF's exhibit the asymmetry mostly at the tails, so that the inverse asymmetry is spread out over the whole core, making it less noticeable.

In summary, the tails of the PDF's give a considerable contribution to the third moment, thus presenting a direct link between the asymmetry (on account of which the third moment does not vanish) and intermittency.

## V. CONNECTION BETWEEN THE DISSIPATION FIELD AND VELOCITY INCREMENTS

It was shown in Sec. III that the intermittency (of the dissipation field) possesses asymmetry. In contrast, Sec. IV relates the asymmetry of the velocity increments, following from the Kolmogorov law, with the PDF's tails, i.e., with the intermittency of the $u$ field. On the other hand, these two fields are related through the RSH (4). As mentioned in Sec. II, there are some deviations from this relationship. We may try to explain some of the deviations related to the asymmetry by a quantitative study of those deviations. In particular, one can compare the experimental value of $\langle|u|\rangle$ with what follows from the RSH, the latter predicting that

$$\langle|u|\rangle_{\mathrm{RSH}}=\langle|V|\rangle\langle y\rangle, \tag{20}$$

by measuring the quantities $\langle|V|\rangle$ and $\langle y\rangle$ directly. Such a comparison of $\langle|u|\rangle$ and $\langle|u|\rangle_{\mathrm{RSH}}$ is given in Fig. 10(a). These curves are quite close to each other. On the other hand, one may consider what we may call the inverse hypothesis, namely, the RSH suggests that $V$ and $y$ are statistically independent, and therefore the statistics of $u$ are related to the statistics of the dissipation field $y$ through the RSH: and that is reflected in Eq. (20). In the inverse case, we assume that $u$ and $y$ are statistically independent, testing this inverse hypothesis experimentally. That is, we define $V=u/y$, then, if $u$ and $y$ are statistically independent,

$$\langle|V|\rangle=\langle|u|\rangle\left\langle\frac{1}{y}\right\rangle, \tag{21}$$

from which it follows that

$$\langle|u|\rangle_i=\frac{\langle|V|\rangle}{\langle 1/y\rangle}, \tag{22}$$

It can be seen from Fig. 10(a) that the experimental $\langle|u|\rangle$ (being quite close to $\langle|u|\rangle_{\mathrm{RSH}}$) is higher than $\langle|u|\rangle_i$. Analogously, one can compare the experimental $\langle|V|\rangle$ with $\langle|V|\rangle_{\mathrm{RSH}}=\langle|u|\rangle/\langle y\rangle$, by Eq. (20), and with $\langle|V|\rangle_i=\langle|u|\rangle\langle 1/y\rangle$ [according to Eq. (21)]. This comparison is depicted in Fig. 10(b). Again, the RSH is satisfied substantially better than the inverse hypothesis.

More detailed information about the first moment is given by the correlation coefficient

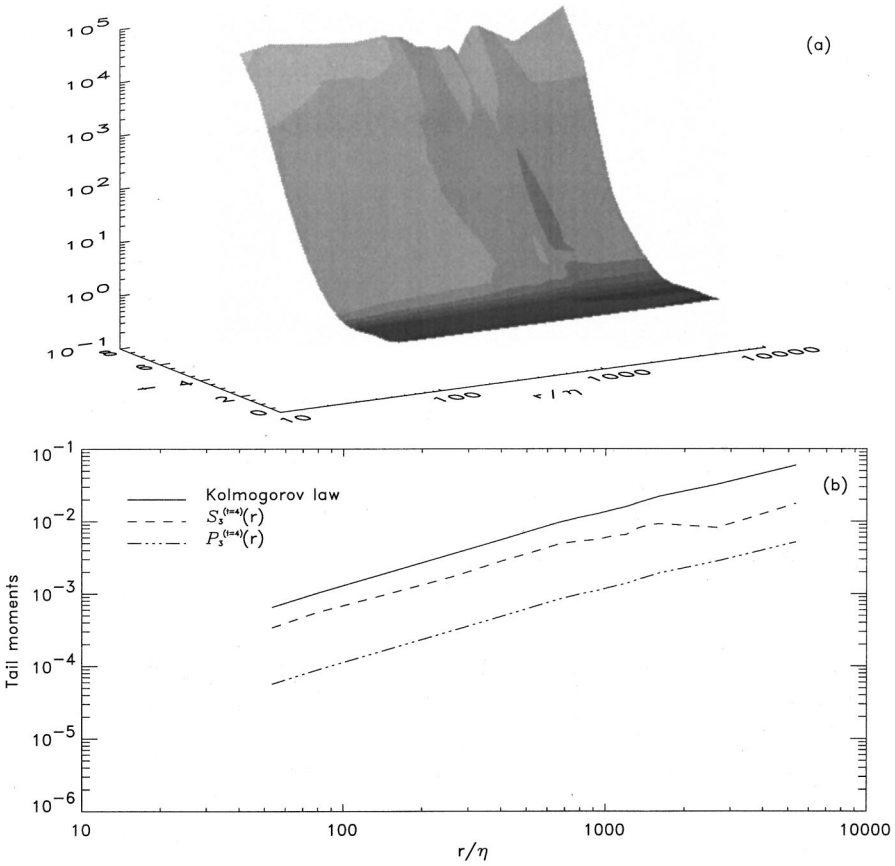


FIG. 8. (a) The ratio $\mathcal{S}_3^{(t)}(r)/\mathcal{P}^{(t)}(r)$ is depicted. For large $t$, where only far tails may contribute, the experimental tail moment is many orders of magnitude higher than the ''ideal'' distribution. (b) Comparison of $\mathcal{S}_3^{(t=4)}(r)$ with $\mathcal{P}^{(t=4)}(r)$, and with the Kolmogorov law.

$$\rho(|u|,y)=\frac{\langle(|u|-\langle|u|\rangle)(y-\langle y\rangle)\rangle}{\sqrt{\langle(m.u|-\langle|u|\rangle)^2\rangle}\sqrt{\langle(y-\langle y\rangle)^2\rangle}}, \tag{23}$$

which should be compared with what follows from the RSH,

$$\rho(|u|,y)_{\mathrm{RSH}}=\frac{\langle|V|\rangle\sqrt{\langle(y-\langle y\rangle)^2\rangle}}{\sqrt{\langle V^2\rangle\langle y^2\rangle-\langle|V|\rangle^2\langle y\rangle^2}}. \tag{24}$$

It can be seen from Fig. 10(c) that the correlation $\rho(|u|,y)$ is relatively high—and this just echoes all previous studies [4]. The coefficient $\rho(|u|,y)_{\mathrm{RSH}}$ is only slightly bigger than $\rho(|u|,y)$. On the other hand, as $V=u/y$ and $y$ are supposed to be statistically independent, the coefficient $\rho(|u|/y,y)$ should vanish. Figure 10(c) shows indeed that the latter is small, in good agreement with the RSH.

In order to make some quantitative estimate, we measure the ratio of these two coefficients, $|\rho(|V|,y)|/\rho(|u|,y)$, depicted in Fig. 10(d). The ratio is small; surprisingly, however, it is not small enough, especially for large distances (where it reaches 0.4 [19]).

In an attempt to interpret all this, we may assume that the deviations from the RSH are described by an additional (small) term in the RSH,

$$u=V'y+\delta u \tag{25}$$

[cf. Eq. (5)], where $V'$ and $y$ are statistically independent as before, and $\delta u$ is statistically independent of $y$ (for other modifications of the RSH see, e.g., [18,5]) We thus suppose that $|\delta u|$ gives only a small contribution to the RSH. Assuming the opposite, that is, that $|\delta u|\gg|V'y|$, would result in the inverse hypothesis, because then $u$ is statistically independent of the dissipation field $y$.

We thus write

$$V=\frac{u}{y}=V'+\frac{\delta u}{y}. \tag{26}$$

If we neglect the first term on the right-hand side (inverse hypothesis), $|V|=|\delta u|/y$, and increasing $y$ would correspond to decreasing $|V|$, and vice versa. This anticorrelation corresponds to a negative correlation coefficient $\rho(|u|/y,y)$; and, indeed, this coefficient is mostly negative [see Fig. 10(c)].

Return to Eq. (26) with small $\delta u$, that is, to the realistic situation. In that case no substantial change in $u$ statistics can be expected. But, in spite of that, the contribution of this correction to the statistics of $V$ could be substantial. Indeed, small values of $y$ would result in large $|\delta u|/y$, thus creating tails in the $V$ distribution. Recall that the tails correspond to rare events, and therefore $\delta u$ does not need to be large in order to give a substantial contribution to the $V$ tails. In addition, because of the noted asymmetry of the dissipation field (see Sec. III), and in view of the above-mentioned anticorrelation between $\delta|u|/y$ and $y$, these tails in the $V$ distribution are expected to possess a ''wrong'' asymmetry. Roughly speaking, $V^+=u^+/y^+$ is greater than $V^-=u^-/y^-$ simply because $y^->y^+$. This might explain the ''wrong'' asymmetry of $V=u/y$ (see Sec. II).

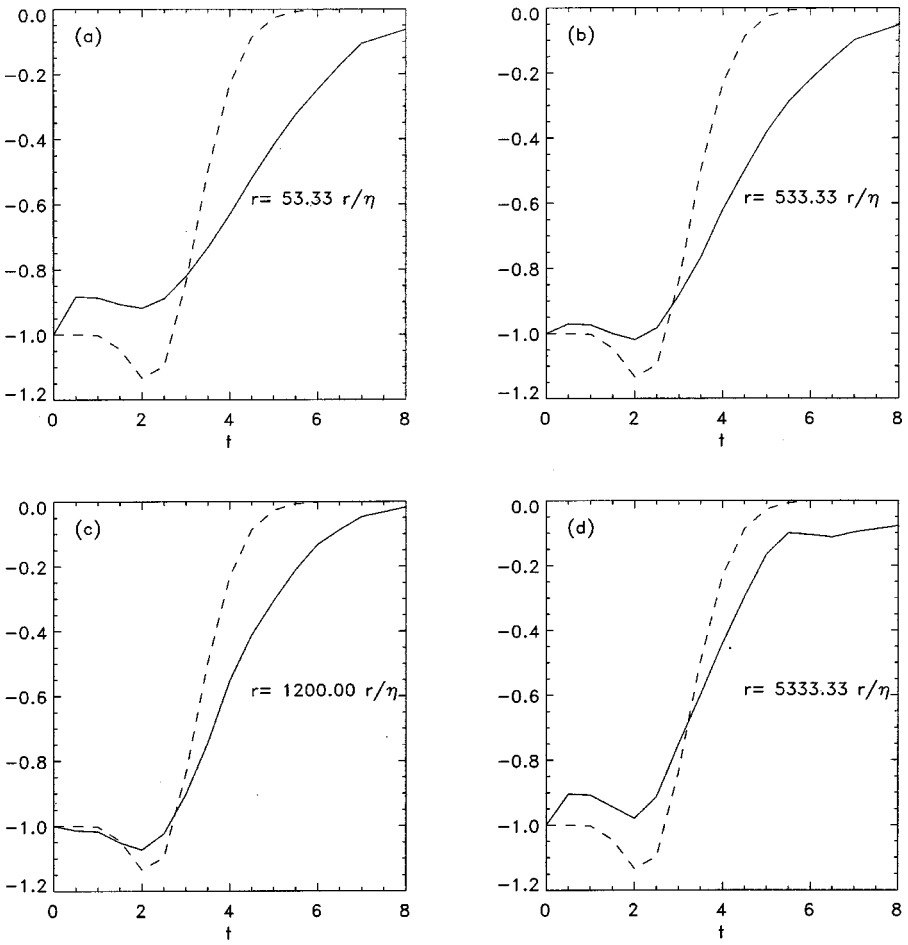


FIG. 9. The tail moments $\mathcal{S}_3^{(t)}(r)$ (solid lines) and $\mathcal{P}^{(t)}(r)$ (dashed lines) are depicted as functions of $t$, for different fixed distances. As in Fig. 7, the moments are normalized to their values at $t=0$.

## VI. CONCLUSION

The asymmetry of turbulence is thus tightly related to the intermittency. On one hand, the intermittency is well established in the dissipation range, or at least, it is most pronounced in this range. It was shown in Sec. III by direct measurements that the intermittency is asymmetric. On the other hand, the asymmetry by itself is known for the velocity increment statistics, following from the Kolmogorov law. We saw in Sec. IV that this asymmetry is manifested mostly

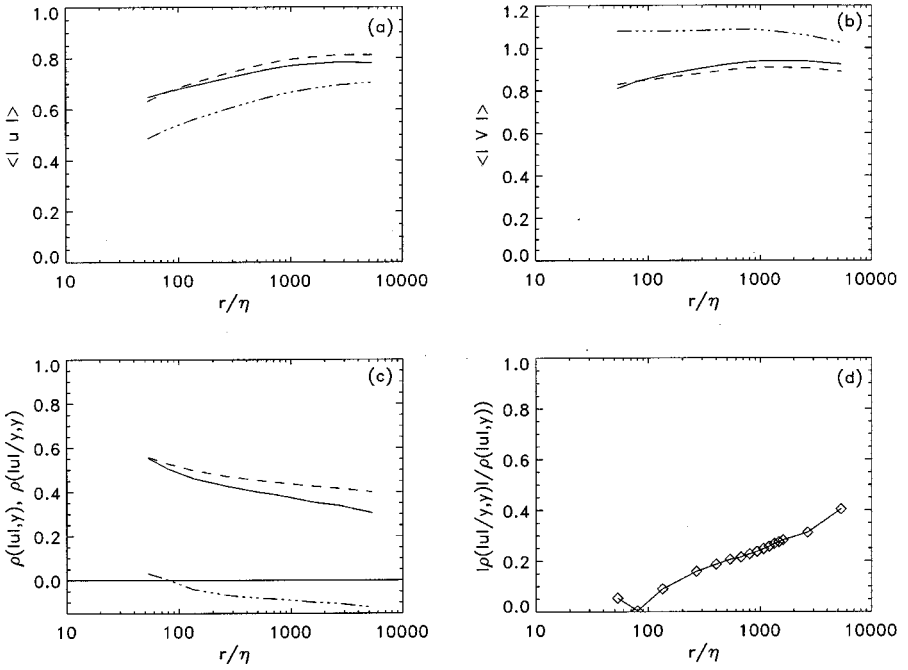


FIG. 10. Comparison of experimental measurements [solid lines in (a)–(c)] with what is predicted by the RSH (dashed lines), and with the assumption that $u$ and $y$ are statistically independent (dash-dotted lines). In particular, the correlation coefficient $\rho(|u|/y,y)$, which is supposed to vanish in the framework of the RSH, is depicted in (c) with the dash-dotted line. (d) depicts the ratio of $|\rho(|u|/y,y)|$ to $\rho(|u|,y)$.

in the tails, relating the asymmetry to the intermittency of the velocity increment statistics.

This link between the Kolmogorov law and the dissipation field is of no surprise, the statistics of the velocity increments being connected with those of the dissipation field via the RSH. In spite of some deviations from the RSH (see, e.g., Sec. V), this hypothesis is well supported experimentally.

The ramp model suggests some explanations for the connection between the asymmetry and intermittency. In spite of some progress achieved in recent years in this respect, it is still unclear what dynamical processes result in this link, so that the ramp model still remains empirical. The present study, we feel, does suggest an approach to this key question. An attempt to address this problem is given below.

According to the classical picture, fully developed turbulence transforms the large scale kinetic energy into the intermediate scales of the inertial range, where it goes into smaller and smaller scales, eventually reaching the dissipation scale where viscous dissipation takes over and destroys the eddies. This cascade of energy is suggested to be self-similar, resulting in specific scaling of the velocity increments [1]. The RSH, on the other hand, suggests that the dissipation is inhomogeneous, and fluctuates from one subvolume to another [2]. As a result, the velocity increments are statistically related to the dissipation field, as in Eq. (4), and the scaling is modified.

The direction of this energy cascade—from large eddies to small ones—is reflected by the Kolmogorov law [6]. i.e., by negative skewness [7]. According to Betchov [20], the production of vorticity is efficient if the symmetric part of the strain tensor results in forming vortex sheets, rather than vortex tubes. In other words, this statistical preference for vortex sheets over vortex tubes corresponds to the asymmetry dictated by the Kolmogorov law. As the latter is satisfied all over the inertial range, we may assume that these vortex sheets (rather than tubes) are formed at each level $r$, as long as the size $r$ corresponds to a subvolume in the inertial range. This hierarchy of vortex sheets of different sizes does not correspond to an intermittency, though, because these structures may be homogeneously distributed over the different subvolumes.

The above scenario implies that the lifetime of an eddy is $r/v_r$, so that the eddy of size $r$ is decaying due to an instability into smaller size eddies, which are still in the inertial range. Suppose now that a vortex is more persistent and it lives somewhat longer. The energy transfer is somewhat suppressed, but not completely. At least, the symmetric part of the strain tensor will generate a vortex sheet, or a tube of a small radius (actually, the first rather than the second), comparable with the Taylor microscale, where the energy is efficiently dissipated due to viscosity. This eddy is thus persistent, forming a coherent structure, and the energy is deposited from the scale $r$ directly to the viscous range without passing through the intermediate scales in the inertial range. The structure thus consists of the initial eddy and the generated thin sheet, resulting in both intermittency and asymmetry. Because of the scale separation between $r$ and the Taylor microscale, where the dissipation takes place, the direct connection between the velocity increments and the dissipation, as in Eq. (4), is broken: because the RSH is formulated for each fixed scale $r$. This may account for the deviations from the RSH, described by the additional term in Eq. (25). The main conclusion of these considerations is that the intermittency and asymmetry are formed simultaneously.

Further studies are needed to confirm or discard the above considerations. It is clear for now, though, that the concept of the ramp model has proved to be useful in interpreting previous experimental results which show some deviations from the RSH. Study of the asymmetry of turbulence seems to be a useful tool in understanding the intermittency, and in constructing a self-consistent picture of fully developed turbulence statistics.

## ACKNOWLEDGMENTS

The main ideas behind experimental studies of turbulence asymmetry were suggested by A. M. Yaglom. I thank K. R. Sreenivasan and B. Dhruva for generously sharing with me the data on atmospheric turbulence used in this paper. I acknowledge discussions with N. Lebovitz.

[1] A.N. Kolmogorov, C. R. Acad. Sci. URSS **30**, 301 (1941).
[2] A.N. Kolmogorov, J. Fluid Mech. **13**, 82 (1962).
[3] K.R. Sreenivasan and R.A. Antonia, Annu. Rev. Fluid Mech. **29**, 435 (1997).
[4] I. Hosokawa and K. Yamamoto, Phys. Fluids A **4**, 457 (1992); A.A. Praskovsky, *ibid.* **4**, 2589 (1992); S.T. Thhoroddsen and C.W. Van Atta, *ibid.* **4**, 2592 (1992); S.T. Thhoroddsen, *ibid.* **7**, 691 (1995); Y. Zhu, R.A. Antonia, and I. Hosokawa, *ibid.* **7**, 1637 (1995); L.P. Wang, S. Chen, J.G. Brasseur, and J.C. Wyngaard, J. Fluid Mech. **309**, 113 (1996); G. Stolovitzky, P. Kailasnath, and K.R. Sreenivasan, Phys. Rev. Lett. **69**, 1178 (1992); G. Stolovitzky and K.R. Sreenivasan, Rev. Mod. Phys. **66**, 229 (1994); S. Chen, G.D. Doolen, R.H. Kraichnan, and Z.-S. She, Phys. Fluids A **5**, 458 (1993); S. Chen, G.D. Doolen, R.H. Kraichman, and L.-P. Wang, Phys. Rev. Lett. **74**, 1755 (1995); V. Borue and S.A. Orszag, Phys. Rev. E **53**, R21 (1996); I. Hosokawa, S. Oide, and K. Yamamoto, Phys. Rev. Lett. **77**, 4548 (1996).
[5] S.I. Vainshtein, Phys. Rev. E **58**, 1851 (1998).
[6] A.N. Kolmogorov, C. R. Acad. Sci. URSS **32**, 16 (1941).
[7] A.S. Monin and A.M. Yaglom, *Statistical Fluid Mechanics* (MIT Press, Cambridge, MA, 1971), Vol. 2.
[8] S.I. Vainshtein and K.R. Sreenivasan, Phys. Rev. Lett. **73**, 3085 (1994).
[9] K.R. Sreenivasan, S.I. Vainshtein, R. Bhiladvala, I. San Gil, S. Chen, and N. Cao, Phys. Rev. Lett. **77**, 1488 (1996).
[10] S.I. Vainshtein, Phys. Rev. E **56**, 447 (1997).
[11] S.I. Vainshtein, Phys. Rev. E **56**, 6787 (1997).
[12] B. Castaing, Y. Gagne, and E.J. Hopfinger, Physica D **46**, 177 (1990); R. Benzi, L. Biferale, G. Paladin, A. Vulpiani, and M. Vergassola, Phys. Rev. Lett. **67**, 2299 (1991); P. Tabeling, G. Zocchi, F. Belin, J. Maurer, and H. Willaime, Phys. Rev. E **53**, 1613 (1996); A. Noullez, G. Wallace, W. Lempert, R.B. Miles, and U. Frisch, J. Fluid Mech. **339**, 287 (1997).
[13] R. Benzi, S. Ciliberto, C. Baudet, F. Massaioli, R. Tripiccione, and S. Succi, Phys. Rev. E **48**, 29 (1993).

[14] G. Stolovitzky, C. Meneveau, and K.R. Sreenivasan, Phys. Rev. Lett. **80**, 3883 (1998).
[15] H.G.E. Hentschel and I. Procaccia, Physica D **8**, 435 (1983).
[16] S.I. Vainshtein, K.R. Sreenivasan, R.T. Pierrehumbert, V. Kashyap, and A. Juneja, Phys. Rev. E **50**, 1823 (1994).
[17] C. Meneveau and K.R. Sreenivasan, J. Fluid Mech. **224**, 429 (1991).
[18] S. Chen, K.R. Sreenivasan, and M. Nelkin, Phys. Rev. Lett. **79**, 1253 (1997); S. Chen, K.R. Sreenivasan, M. Nelkin, and N. Cao, *ibid.* **79**, 2253 (1997).
[19] The experimental coefficient $\rho(|V|,y)$ is not exactly zero even if $V$ and $y$ are statistically independent. Simple estimation suggests that, in this case, $\rho(|V|,y)\approx 1/N^{1/2}$, where $N$ is the number of events. For the large arrays that we are dealing with, this coefficient would be $3\times 10^{-4}$, which is well below the number given in Fig. 10(c).
[20] R. Betchov, J. Fluid Mech. **1**, 497 (1957).